Top Catal (2008) 47:73–83
DOI 10.1007/s11244-007-9035-2

ORIGINAL PAPER

Electrodeposited Metals at Conducting Polymer Electrodes. II: Study of the Oxidation of Methanol at Poly(3-methylthiophene) Modified with Pt–Pd Co-catalyst

Ahmed Galal · Nada F. Atta · Soher A. Darwish · Shimaa M. Ali

Published online: 26 February 2008

Abstract The electrodeposition of sub-micro/nano-size Pt–Pd co-catalyst on conducting poly(3-methylthiophene) (PMT) films and the use of the resulting hybrid material for the oxidation of methanol are reported. Several factors affecting the electrocatalytic activity for this process were studied by cyclic voltammetry (CV) and electrochemical impedance spectroscopy (EIS), namely, the polymer film thickness, and the catalyst amount/ratio. In addition, the effects of methanol concentration and the operating temperature were also investigated. Thermal gravimetric analysis (TGA) showed that the thermal stability of the polymer film increased by the incorporation of the metallic particles. Scanning electron micrographs (SEM) were obtained to identify the relative size of the metallic particles and their distribution. The size ranged between 3 μm and 500 nm. Energy dispersive X-rays analysis (EDAX) was performed to identify the composition of the metallic particles. It was found that the particle composed of Pt and Pd in ratio that is comparable to that present in the feed solution.

Keywords Conducting polymers · Nano-sized catalyst · Pt–Pd alloy · Methanol oxidation · CV · EIS · TGA · SEM · EDAX

1 Introduction

In the last few years, the synthesis and characterization of nano-sized metal particles has attracted a lot of interest [1] because of their possible use in technologically relevant applications, particularly in the field of enhanced performance catalysts [2–4]. In order to employ these nanoparticles as active elements in a device, issues on how to support them have to be faced. A proper choice seems to be that of embedding or depositing the particles on a polymer, several examples have been already proposed [5, 6].

Studies on the electrocatalytic oxidation of methanol on metal surfaces indicate the viability of using methanol in liquid fuel cells [7, 8]. Methanol is non-toxic, easy to store and handle, operates at relatively moderate temperatures and posses high energy density. One of the most commonly used metal surfaces is bulk Pt, whose use is justified by the activity and stability of Pt in aqueous acidic solutions [7, 8]. Platinum is known to activate the dissociative adsorption of methanol at an appreciable rate. However, it is well known that some intermediate products of the reaction are strongly adsorbed at the electrode surface that causes poising to the surface such as CO_{ad} and leading to a loss of the electrocatalytic activity of the electrode. To enhance the efficiency of bulk Pt and to reduce costs, novel electrode materials are prepared by modifying base Pt or GC with metallic nanoparticles, e.g. Pt and Pt alloys supported on a polymer matrix. These electrodes exhibit enhanced electrocatalytic activities as compared with the bulk-form metal electrodes in the oxidation of small organic molecules and was studied earlier [9–23]. The increase in the catalytic activity may be due to the decrease in the poisoning effect, which is caused by highly dispersed single metal [10–17], bi-metals [18–22] or multi-metals [20–23] and the synergistic effects of conducting polymer and metal particles [24, 25]. The metallic particles can be supported on a polymer matrix through two main types of procedures: the catalyst particles are incorporated into the

A. Galal (✉) · N. F. Atta · S. A. Darwish · S. M. Ali
Department of Chemistry, Faculty of Science, University of Cairo, 12613 Giza, Egypt
e-mail: galalah@chem-sci.cu.edu.eg

polymer film during the electropolymerization of a suitable monomer from a solution containing both monomer and a metallic precursor salt, or the catalyst particles are electrodeposited on a previously prepared polymer film using a solution containing a metallic precursor salt. The first procedure normally yields embedded metal particles that are less accessible to species in solution. On the other hand, the electrochemical deposition of metal particles can be carried out by several ways such as constant potential, double potential step and cyclic potential mode. It was found that the electrocatalytic behavior of the Pt deposited by different electrochemical methods was slightly different, perhaps reflecting a different distribution (2D or 3D) or state (crystalline or grain morphology) of the metals deposited. Kelaidopoulou et al. [20] found that Pt particles deposited by constant potential method are almost homogeneously dispersed over the polymer matrix. The cyclic potential method enables the deposited metal particle to activate periodically and improve their dispersion [15, 17]. As for the double potential step method, it has the advantage to improve the penetration of the $[PtCl_6]^{2-}$ complex into the conducting polymer film, which is believed to result in a 3D Pt catalyst distribution [10] and Pt crystallites with preferential crystallographic orientation [16].

In this work, PMT was used as a support for sub-micro/nano-sized Pt–Pd particles and the resulting hybrid material was employed as a catalyst for oxidation of methanol. Several factors affecting the catalytic activity will be studied such as the polymer film thickness, the catalyst amount/size/distribution and the catalyst ratio, methanol concentration and the operating temperature. Moreover, thermal and surface analyses will be presented.

2 Experimental

2.1 Chemicals and Reagents

All chemicals were used as received without further purification. 3-Methylthiophene (MT), N-Methylpyrrole (NMPy), tetrabutyl ammonium hexafluorophosphate (TBAHFP), acetonitrile (AcN), perchloric acid, hydrochloric acid, nitric acid, sulfuric acid and methanol were obtained from Aldrich (Milwaukee, USA). Platinum (II) chloride (Cambridge Chemicals, Oxford England) and palladium (II) chloride (Scherimg Kaul Paum AG, Berlin Germany) were also used. Aqueous solutions were prepared using double-distilled water.

2.2 Electrochemical Cells and Equipments

Electrochemical polymerization and characterizations were carried out in a three-electrode/one-compartment glass cell. The working electrode was a platinum disc (diameter: 1.5 mm), or glassy carbon disc (diameter: 3.0 mm). The auxiliary electrode was in the form of 6.0 cm platinum wire. All the potentials in the polymerization, the voltammetric studies, and the electrochemical impedance spectroscopic measurements were referenced to a saturated Ag/AgCl electrode. All working electrodes were mechanically polished using an alumina (2 μm)/water slurry until no visible scratches were observed. Prior to immersion in the cell, the electrode surface was thoroughly rinsed with distilled water and dried. All experiments were performed at 25 °C.

The electrosynthesis of the polymers and their electrochemical characterization were performed using a BAS-100B electrochemical analyzer (BAS, West Lafayette, USA). EIS measurements were performed using a Gamry-750 system and a lock-in-amplifier. The data analysis software was provided with the instrument and applied nonlinear least square fitting with Levenberg-Marquardt algorithm. All impedance experiments were recorded between 0.1 Hz and 100 KHz with an ac excitation signal of 5 mV amplitude. Thermal gravimetric analysis was performed using a Shimadzu TGA-50H instrument. Heating rate was 10 °C/min and inert gas used was purified nitrogen. Philips XL 30 instrument was used to obtain the scanning electron micrographs of the films.

2.3 Preparation of Platinum (II) Chloride/Palladium (II) Chloride Solution

Each of the platinum (II) chloride and palladium (II) chloride salts were dissolved in hot aqua regia. The formed solution was heated until one-fourth of the original volume was reached by evaporation. The remaining solution was diluted to the required volume and concentration using 0.1 M perchloric acid. The final solutions thus prepared were used to prepare the mixed co-catalyst as will be indicated later.

3 Results and Discussion

3.1 Deposition of the Catalyst on PMT

The electropolymerization of MT can be achieved by applying a constant potential between the platinum disc-working electrode and the reference Ag/AgCl (+1.8 V) for a given time. The thickness of the resulting polymer film is therefore controlled by the time elapsed during the electrolysis step. The synthesis solution consisted of 0.05 M MT and 0.05 M TBAHPF dissolved in dry AcN. The preparation of the polymer was followed by an

electrochemical deposition of the catalyst on the polymer film. Thus, the polymer film was immersed in $PtCl_2/PdCl_2$ solution and a double potential step was applied to the polymer as follows $E_1 = 0$ V for 30 s and $E_2 = +0.1$ V for 600 s (or as indicated).

3.2 Catalytic Oxidation of Methanol

The electrochemical reaction of Pt in sulfuric acid involves adsorption of hydrogen, formation of platinum oxide, oxidation of hydrogen and reduction of platinum oxide [26]. The formation of hydrogen atoms takes place around +0.18 V, and hydrogen evolution starts at −0.17 V, while formation of platinum oxide takes place at about +0.62 V and its reduction at +0.55 V [27]. Figure 1 shows the cyclic voltammograms of different surfaces modified with sub-micro/nano-structured Pt/Pd co-catalyst in 0.5 M methanol + 0.1 M H_2SO_4 solution. The substrate surfaces studied are Pt, GC and PMT electrodes. In all cases, the co-catalyst was electrodeposited according to the following procedure: applying 0.0 V to the working electrode for 30 s then 0.1 V for 600 s from a feed solution containing Pt:Pd in ratio 3:1. Two peaks corresponding to methanol oxidation can be identified in the potential range between +0.4 V and +1.2 V that were observed for other substrates and catalysts in the literature [28]. However, the position of the oxidation potential changes according to the type of substrate onto which the co-catalyst was deposited. The current recorded for the oxidation process and reduction peak was in the order of PMT–(Pt/Pd) > Pt–(Pt/Pd) > GC–(Pt/Pd). The conducting polymer is obviously showing superior electrocatalytic efficiency for methanol oxidation. No current peaks were observed for PMT in the methanol containing acidified aqueous solution. This indicates that the conducting polymer film shows no electrocatalytic activity for methanol oxidation.

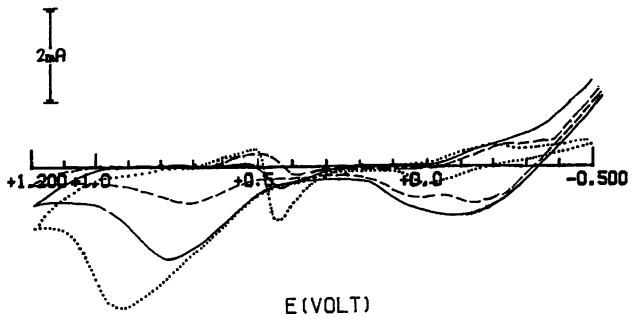

Fig. 1 Cyclic voltammograms of different surfaces modified with sub-micro/nano-(Pd/Pt, 1:3) particles in 0.5 M methanol/0.1 M H_2SO_4/H_2O. (˜) Pt, (—) GC, and (....) GC/PMT electrodes. Scan rate = 50 mV s^{-1}, $E_i = -0.5$ V, $E_f = +1.2$ V, 10th cycle only shown

3.3 Effect of Polymer Thickness on Electrocatalytic Activity

Figure 2 shows the effect of changing the polymer film thickness on the electrocatalytic oxidation of methanol. As could be observed, the current corresponding to the methanol oxidation (peak I) is relatively higher for thinner films. It is clear that as the film thickness increases its electronic resistance increases and should therefore hinder the charge transfer (cf. Fig. 2b). At this stage, and taking into account the following intermediates formed during the oxidation step [27]:

$$(CH_3OH)_{ads} \rightarrow (CH_3O)_{ads} + H^+ + e^-$$

$$(CH_3O)_{ads} \rightarrow (CH_2O)_{ads} + H^+ + e^-$$

$$(CH_2O)_{ads} \rightarrow (CHO)_{ads} + H^+ + e^-$$

$$(CHO)_{ads} \rightarrow (CO)_{ads} + H^+ + e^-$$

The above processes are represented by the appearance of the anodic peak (I). This is followed by a decrease in current that expresses the formation of platinum oxide according to [29]:

$$Pt + H_2O \rightarrow PtO + 2H^+ + 2e^-$$

Further increase in current is due to the formation of CO_2 on the surface of platinum oxide. In the reverse scan, a reduction peak appears (II) due to the reduction of platinum oxide according to:

$$PtO + 2H^+ + 2e^- \rightarrow Pt + H_2O$$

Further oxidation takes place with the appearance of peak (III) on a rather reduced/non-poisonned Pt surface [27].

3.4 Effect of Co-catalyst Loading on the Substrate on the Electrocatalytic Oxidation of Methanol

The amount of co-catalyst deposited on the conducting polymer film increases with time passed when the potential was held at 0.1 V for 1, 3, 7 and 10 min, respectively. As expected, the catalytic efficiency for methanol oxidation increases with the amount of co-catalyst. These results, shown by Fig. 3 are explained in terms of increase in the surface area of the co-catalyst. The morphology and size of co-catalyst should also affect the electrocatalytic conversion efficiency.

3.5 Effect of Catalyst Deposition Voltage and Working Temperature

Figure 4 shows the effect of changing the potential of co-catalyst deposition. The increase in the positive limit between +0.1 and +0.3 V results in a decrease in the

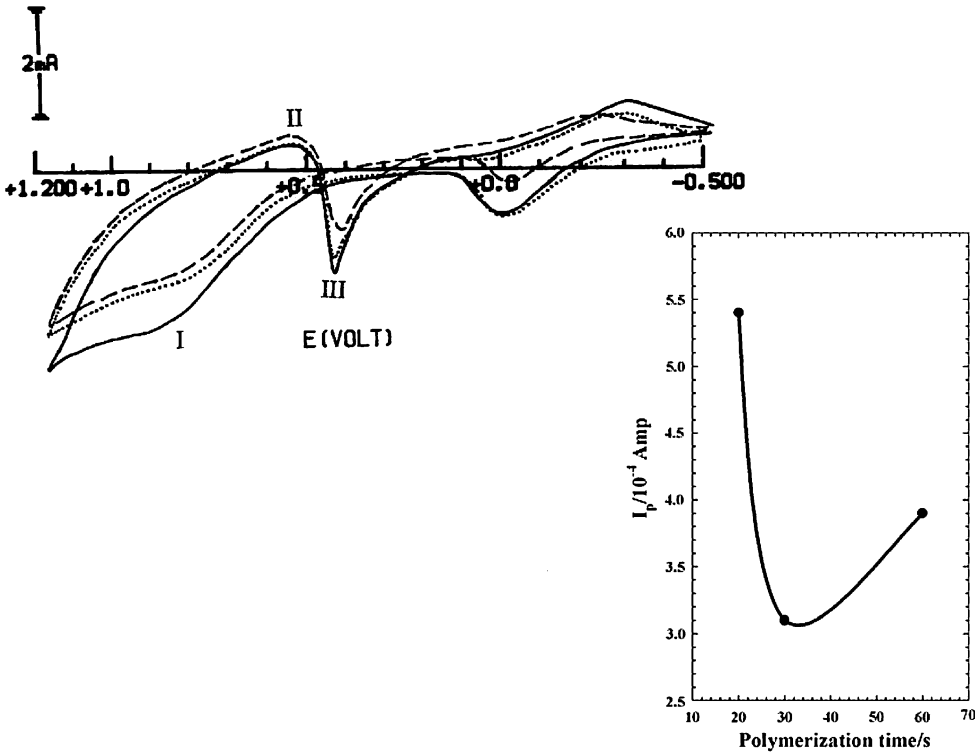

Fig. 2 Cyclic voltammograms of PMT films (formed from 0.05 M MT/0.05 M $TBAPF_6$/AcN, $E_{app.} = +1.8$ V with different deposition times (—) 20 s, (- - -) 30 s, and (....) 60 s on GC) modified with sub-micro/nano-(Pd/Pt, 1:3) particles (second $E_{app.} = 100$ mV for 10 min) in 0.5 M methanol/0.1 H_2SO_4/H_2O. Scan rate = 50 mV s^{-1}, $E_i = -0.5$ V, $E_f = +1.2$ V, 10th cycle only shown

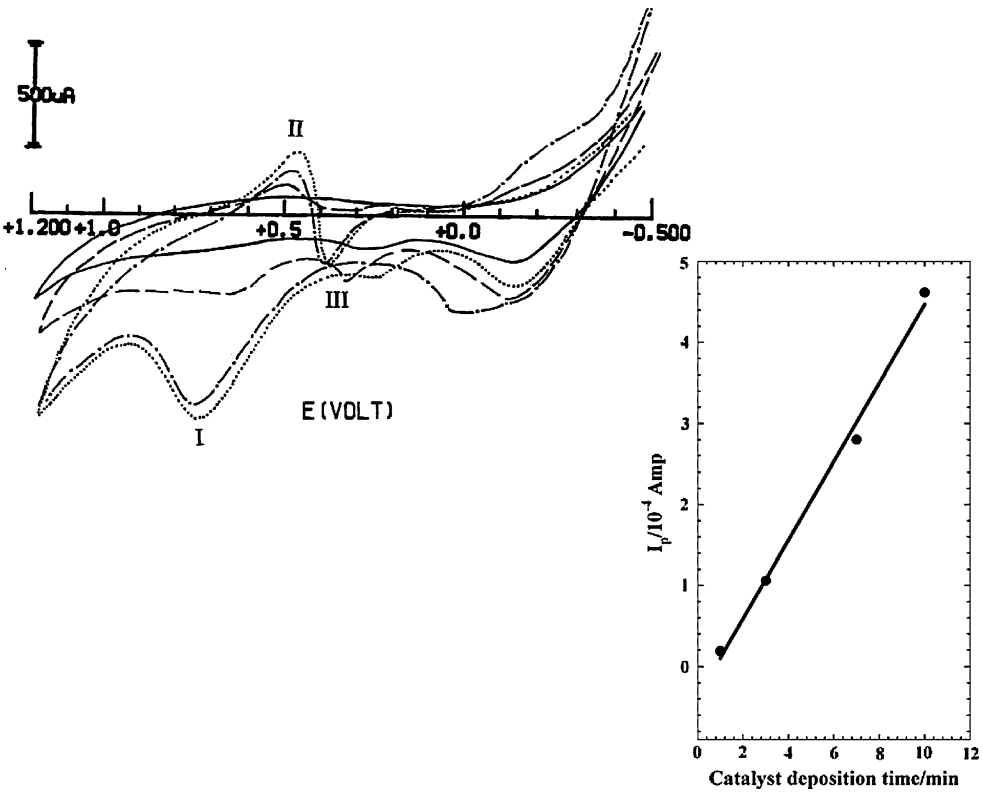

Fig. 3 Cyclic voltammograms of PMT prepared as in Fig. 2 for 30 s on Pt showing effect of varying the time of second deposition potential ($E_{app.} = 100$ mV) for co-catalyst (Pd:Pt 1:3), (—) 1 min, (- - - -) 3 min, (-•-•-) 7 min, and (....)10 min, in 0.5 M methanol/0.1 H_2SO_4/H_2O. Scan rate = 50 mV s^{-1}, $E_i = -0.5$ V, $E_f = +1.2$ V, 10th cycle only shown

current due to methanol oxidation. The increase in the "second" potential step should result in catalyst oxidation rather than increasing its amount/size.

For the purpose of direct methanol fuel cell (DMFC) applications, it would be advisable to study the effect of changing the working temperature for the metal-modified

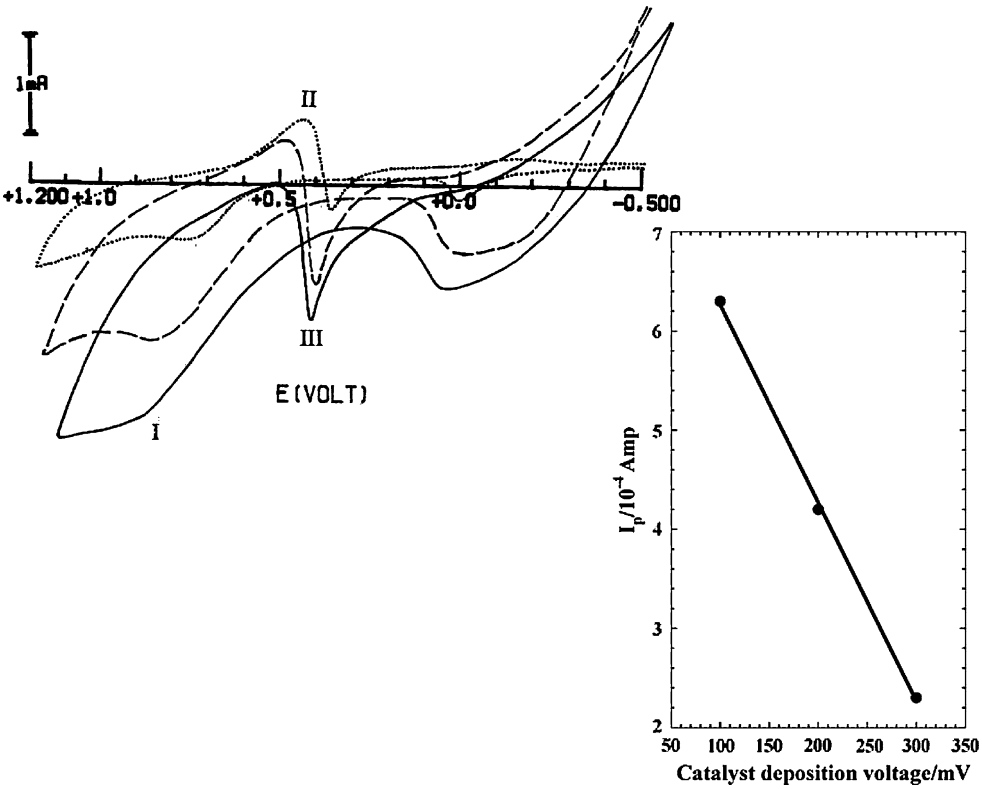

Fig. 4 Cyclic voltammograms of PMT prepared as in Fig. 2 for 30 s on GC modified with sub-micro/nano-(Pd/Pt, 1:3) particles for 10 min at second deposition potential, $E_{app.}$ = 100 mV (—), 200 mV (- - -) and 300 mV (....) in 0.5 M methanol/0.1 H_2SO_4/H_2O. Scan rate = 50 mV s^{-1}, E_i = −0.5 V, E_f = +1.2 V, 10th cycle only shown

conducting polymer films. Figure 5 shows the CV for GC/PMT/Pd:Pt (1:3) tested in 0.1 M Methanol/0.5 M H_2SO_4 at 20, 25, 30, 35 and 40 °C. It is clear that these sub-micro/nano-metal modified polymeric films can be used efficiently at the studied temperature range. However, maximum current was obtained for working temperature of 30 °C. It is suggested that for relatively higher temperatures the adsorption of methanol onto Pt is hindered and became rate determining step. On The other hand, as the concentration of methanol increases the oxidation peak (I) increases and the second peak (II) in the reverse scan also increases with a shift in the positive direction as shown in Fig. 6.

3.6 Effect of Co-catalyst Composition

The effect of changing the ratio of Pt to Pd in the deposition bath solution on the electrocatalytic properties was also studied. The concentration ratio of Pd:Pt was changed according to (1:x, x = 1, 2, 3, 7, 10). The electrochemical oxidation of methanol on the GC/polymer/Pt–Pd has been investigated by CV. The variation of the oxidation peak current for methanol oxidation and the corresponding peak potentials are shown in Fig. 7. In general, as the Pt content increases the oxidation peak potential shifts to negative values. These data implies that the electrooxidation of methanol is facilitated as the Pt content in the co-catalyst increases. The current density increases with the increase of Pd content and then decreases again. The maximum is found when the Pd:Pt ratio is 1:3. Compared to pure Pt, the inclusion of Pd improves the catalytic activity of the catalyst. As in the case of ruthenium [30], Pd provides additional sites for the adsorption of oxygenated species, namely CO_{ads} oxidation. However, as the Pd content increases further decrease in the electrocatalytic activity is observed. This is due to the fact that Pd has no catalytic activity for the electrooxidation of methanol. These two opposing effects result in a maximum current for the Pd:Pt ratio 1:3 in the co-catalyst deposition.

It is important to mention that the modified film is relatively stable for successive cycling in the acidic methanol up to about 50 cycles. The observed decrease in current value for the oxidation process for the last cycle is about 2% compared to that of the first cycle.

3.7 Effect of the Nature of the Polymeric Film on the Electrocatalytic Activity

In a previous study, a series of copolymers of MT and NMPy were prepared from feed solutions containing different ratios of the two monomers. The characterization of the prepared copolymers was carried out by CV and chronocoulometry (CC) in the monomer free solution and diffusion coefficients were calculated for the different films

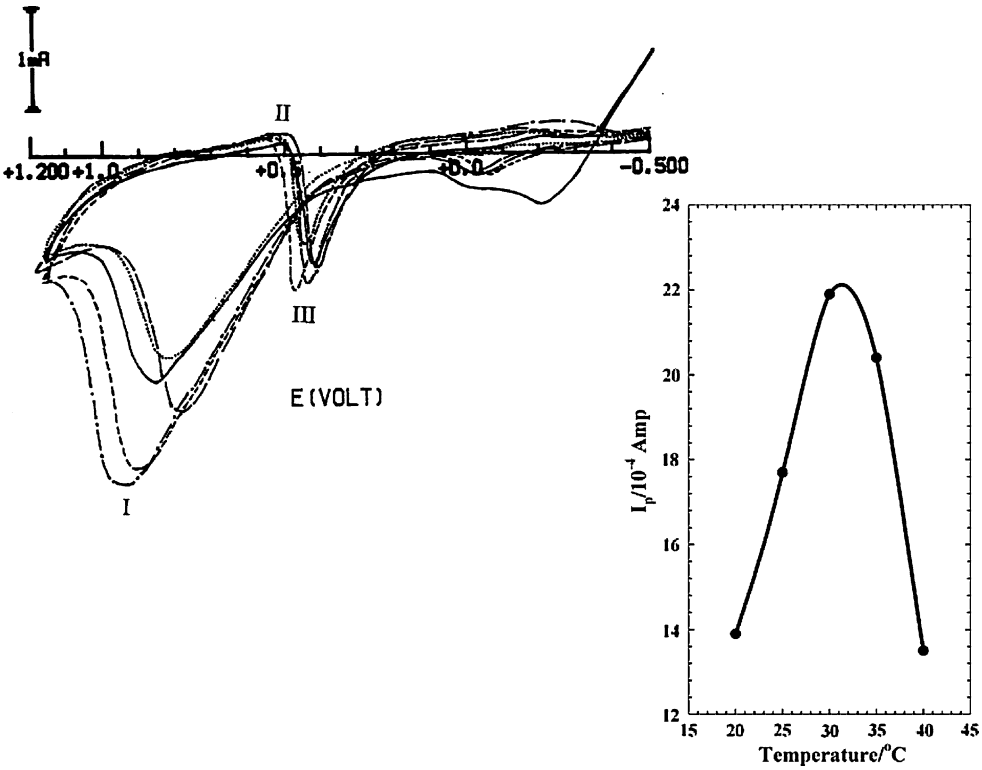

Fig. 5 Cyclic voltammograms of PMT prepared as in Fig. 2 for 30 s on GC modified with sub-micro/nano-(Pd/Pt, 1:3) particles (second $E_{app.}$ = 100 mV for 10 min) in 0.5 M methanol/0.1 H_2SO_4/H_2O. At 20 °C (—), 25 °C (- - - -), 30 °C (-•-•-), 35 °C (- - - -), 40 °C (....). Scan rate = 50 mV s^{-1}, E_i = − 0.5 V, E_f = +1.2 V, 10th cycle only shown

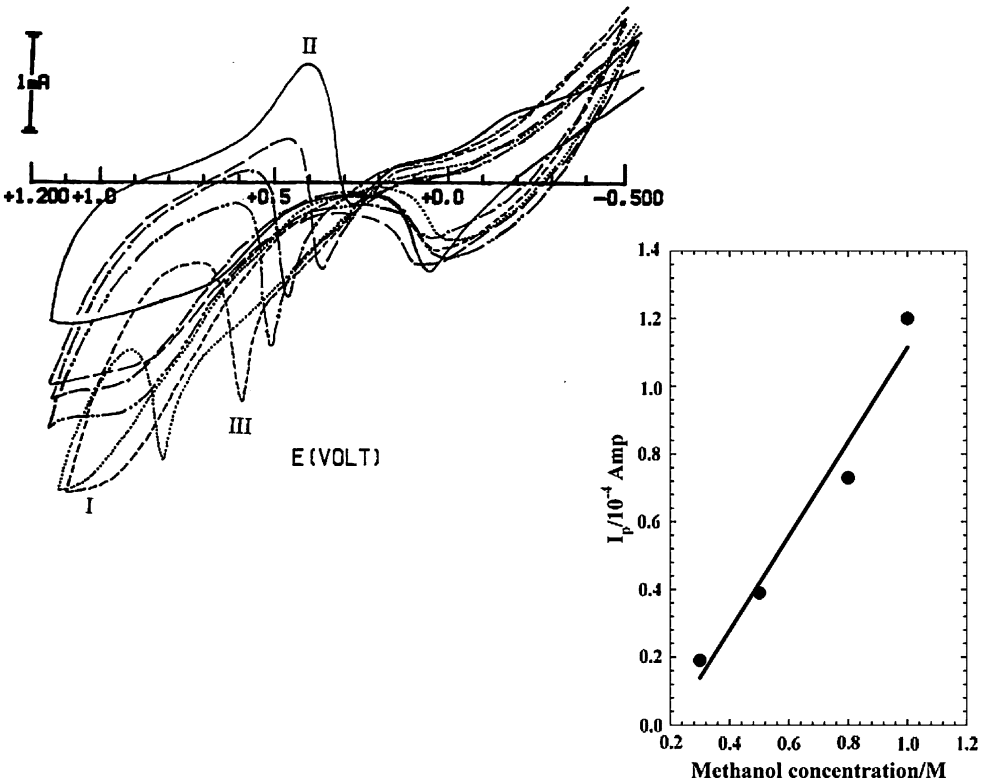

Fig. 6 Cyclic voltammograms of PMT prepared as in Fig. 2 for 30 s on GC modified with sub-micro/nano-(Pd/Pt, 1:3) particles (second $E_{app.}$ = 100 mV for 10 min) in different methanol concentrations 0.1 M (—),0.3 M (- - - -), 0.5 M (-•-•-), 0.8 M (-••-••-), 1 M (- - - -), and 2 M (....). Scan rate = 50 mV s^{-1}, E_i = − 0.5 V, E_f = +1.2 V, 10th cycle only shown

and compared to those calculated for homo-PMT and homo-PMPy. It was found that the copolymer prepared from a feed solution containing MT:NMPy ratio of 9:1 showed unique characteristics that were similar in trend to that of homo-PMT. The most important feature was the trend in increase in the diffusion coefficient values with thickness. Moreover, the morphology characteristics of the copolymer compared to that of the homo-PMT and

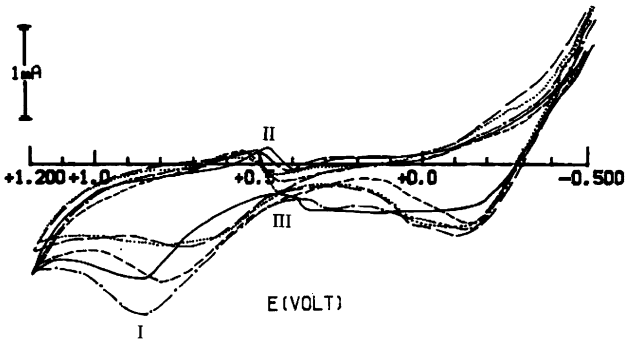

Fig. 7 Cyclic voltammograms of PMT prepared as in Fig. 2 for 30 s on Pt modified with sub-micro/nano-(Pd/Pt) particles in ratios (1:1) (—), (1;2) (- - - -),(1:3) (-•-•-), (1:7) (- - - -), and (1:10) (....) (second $E_{app.}$ = 100 mV for 10 min) in 0.5 M methanol/0.1 H_2SO_4/H_2O. Scan rate = 50 mV s^{-1}, E_i = −0.5 V, E_f = +1.2 V, 10th cycle only shown

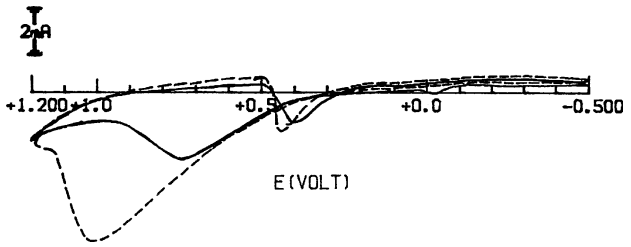

Fig. 8 Cyclic voltammogram of PMT (—) and co(MT/NMPy, 9:1) (- - - -), ($E_{app.}$ = +1.8 V, for 30 s), each modified with sub-micro/nano-(Pd/Pt, 1:3) particles (second $E_{app.}$ = 100 mV for 10 min), in 0.5 M methanol/0.1H_2SO_4/H_2O. Scan rate = 50 mV s^{-1}, E_i = −0.5 V, E_f = +1.2 V, 10th cycle only shown

homo-PNMPy might be advantageous when used as substrate for the submicro-/nano-structured alloys for the oxidation of methanol. Figure 8 shows a comparison between the cyclic voltammetric responses of a copolymer film, homo-PMT films modified with the co-catalyst for the electrochemical oxidation of methanol in acidic solutions. As could be noticed the best electrolytic efficiency for methanol oxidation was that recorded for the copolymer modified with the submicro-/nano-structured catalyst. The "synergistic" effect caused by the polymer film and the catalyst is more pronounced with the copolymer than for PMT. At this point, it is suggested that the surface of the polymer film, in presence of the catalyst, is contributing to the mechanism of methanol oxidation and its morphology, hydrophobic/hydrophilic character and electrical conductivity affects its electrocatalytic efficiency.

3.8 Electrochemical Impedance Spectroscopy (EIS) Studies

Electrochemical impedance spectroscopy data were obtained for PMT modified with submicro-/nano-structured metal alloys at ac frequency varying between 0.1 Hz and 100 kHz with an applied potential in the region corresponding to the electrolytic oxidation of methanol in 0.1 M H_2SO_4. Several factors affecting the electrochemical process were studied namely, the amount of catalyst deposited over the polymer substrate, the polymer film thickness, the temperature of the methanol containing solution.

The data of Fig. 9 shows the change of EIS spectra with the amount of co-catalyst deposited. The corresponding electrochemical parameters are given in Table 1 from the fitting of experimental data to the equivalent circuit of Fig. 10. We followed a non-linear complex minimum square fitting protocol that is well established for studying polymeric systems to calculate the different electrochemical parameters [31]. In our treatment R_s, R_2, C_{dl}, and CPE represent bulk resistance, polarization resistance, double layer capacitance, and a constant phase element, respectively. It could be noticed that the differences in calculated values of R_s for each film changes with amount of catalyst deposited. This indicates that R_s does not represent the electrolytic resistance only. On the other hand, R_2, the charge transfer resistance associated with the interface between polymer and electrolyte or polymer/metal substrate. Whereas, CPE, the constant phase element represents charge accumulation at the interface that, forms the interfacial double layer. The later consideration assumes a flat configuration for the film, i.e. surface roughness is not taken into account. Eventually, the value of CPE is much larger than that corresponding to the double layer. It was experimentally established that the impedance (associated with the constant phase element),

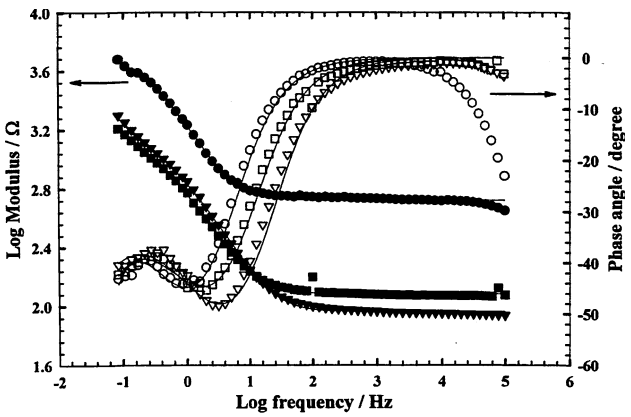

Fig. 9 The Bode plots of impedance spectra obtained, at +0.6 V, for PMT(prepared from 0.05 M MT/0.05 M $TBAPF_6$/AcN by applying +1.8 V for 30 s) coated with different amounts of co-catalyst (Pd:Pt 1:3) (by varying the time of second deposition potential ($E_{app.}$ = 100 mV) for co-catalyst), (•) 3 min, (▼) 7 min, and (□) 10 min, in 0.5 M methanol/0.1H_2SO_4/H_2O. Closed symbols represent log Z versus log f and open symbols represent Phase angle versus log f relations. Solid lines represent simulated data based on the parameters of equivalent circuits of Fig. 10

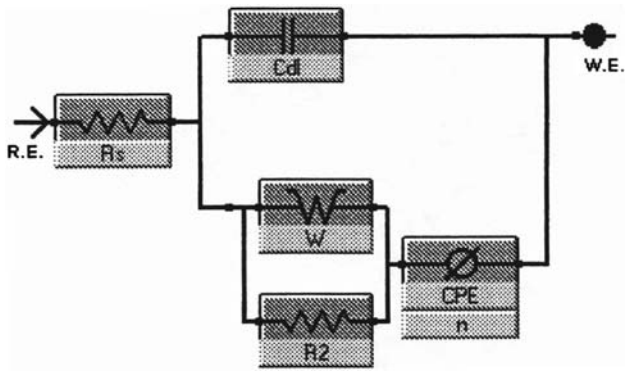

Fig. 10 Equivalent circuits used in the fit procedure of the impedance spectra. The results were analyzed using Levenberg-Marquardt/Simplex algorithms based on a complex non-linear least-squares procedure

Z_C, representing double-layer charging depends on the frequency according to [32]:

$$Z_C = \frac{1}{Q(i\,\omega)^{n_f}} \qquad (n_f < 1) \qquad (1)$$

This phenomenon was observed so widely that it became known as the "constant phase element" that refers to the fact that the complex-plane plot of Z_C is a straight line rotated by an angle φ,

$$\varphi = \left(\frac{\pi}{2}\right)(1 - n_f) \qquad (2)$$

Q is the empirical "CPE-coefficient" and is proportional to $\kappa^{(1-n)}{}_f C_d n_f$ where κ and C_d are the specific conductivity of the electrolytic solution and double layer capacitance, respectively. Examination of the data of Table 1 shows the following:

- The value of R_s generally decreases with the amount of co-catalyst deposited indicating an increase in the film conductivity at the interface. It is important to take into consideration that at this particular applied potential, ca. +0.6 V versus Ag/AgCl, the polymer film is conducting. Moreover, the contribution of ionic diffusion cannot be also ignored.
- The charge transfer resistance, R_2, generally decreases as the amount of co-catalyst increases. It is also important to notice that for co-catalyst deposited for 10 min showed unexpectedly lower values of R_2 and higher ones for R_s. This is explained with the fact that electron transport through the polymer chains is accompanied by ionic migration. As the amount of catalyst increases the polymer coverage area increases that prevents its contribution from ionic diffusion. The transport of the ions through the double layer and particularly at the polymer/solution interface may be modelled as the charge/discharge of a capacitor. Since the surface of the polymer is not ideally regular and binding sites of ions to the polymer possess different energies, a capacitive component and constant phase elements have to be associated with the charge transfer resistance [33].
- It is clear that the CPE is associated with the double layer capacitance, C_{dl} and depends on the amount of co-catalyst used for modification. Thus, the value of CPE decreases while that of C_{dl} increases. The variation of the double layer capacitance produced by charge accumulation at the polymer/solution interface is related to the charge compensation taking place within the electrical double layer during the oxidation process. However, we would expect the results reported in this work to be relatively higher than those reported in the literature [34], due to the difference in estimation of thickness of the film and the method of its formation/modification.
- The Warburg element represents the diffusion through the polymer film. This case is true when diffusion takes place in a medium where the interface precludes the flow of the species and is represented by a hyperbolic tangent function. The value attributed to the element "W" increases with the amount of co-catalyst in the film.

The EIS data gave the effect of changing the thickness of the film with the same amount of co-catalyst and are not shown. The corresponding electrochemical parameters derived from the equivalent circuit of Fig. 10 are given in Table 2. The following observations are made:

- The polarization resistance, R_2, increases with film thickness while the corresponding R_s values decreases. This shows that ionic conduction that should increase with polymer film thickness, contributes to the R_s values.

Table 1 The electrochemical parameters, corresponding to Fig. 9, estimated from the fitting of experimental data to the equivalent circuit of Fig. 10

Time/min	R_s	C_{dl}	W	R_2	CPE	n
3	529.0	6.35×10^{-5}	7,343	7,755	842.1	1.34
7	92.1	8.26×10^{-5}	2,488	1,553	630.5	0.74
10	121.7	12.34×10^{-5}	2,164	1,806	399.6	0.95

Table 2 The electrochemical parameters, corresponding to EIS data for effect of thickness, estimated from the fitting of experimental data to the equivalent circuit of Fig. 10

Time/s	R_s	C_{dl}	W	R_2	CPE	n
20	122.0	12.34×10^{-5}	2,164	1,806	399.6	0.95
30	70.0	10.55×10^{-5}	1,484	4,627	7.7	0.66

- The Warburg component and the capacitance associated with the constant phase element decrease with the increase in the film thickness.
- The double layer capacitance, C_{dl} reported here 123 and 105 μF/cm^2 calculated for the two films, respectively, are relatively higher for similar systems in the same potential ranges [35]. This is explained in terms of the type of redox reaction taking place in this case, namely the oxidation of methanol versus the anion exchange during the doping/undoping process.

The EIS spectra were also measured at the GC/PMT-co-Pt:Pd electrode for the oxidation of methanol at E_{appl} = +0.6 V at different temperatures, 20, 25, and 30 °C, respectively. The corresponding electrochemical data are reported in Table 3. In general, the R_s values increase with temperature indicating the increase in the rate of methanol oxidation resulting in an increase in the concentration of oxidative products that insulates partially the electrode surface. As expected the C_{dl} values, on the other hand, decrease with increase in temperature. And the charge transfer resistance decreases indicating the ease of the oxidation of process at elevated temperatures. However, a resistive component is associated with the constant phase element with n values approaching 2. The Warburg component however, shows a decrease with temperature that reflects the change in the contribution of diffusion with the change in the energy states at the film/electrolyte interface.

3.9 SEM of the Modified Polymer Films

Figure 11 shows the scanning electron micrograph for a polymer film modified with the sub-micro/nano-structured Pt/Pd alloy. A dark phase represents the organic polymer layer and the shiny spots are the sub-micro/nano-metallic particles. A larger magnification of the scanning electron micrograph, Fig. 12, is obtained to identify the size of the metallic particles and it is ranging between 3 μm and 500 nm. At larger magnification, it was found that the particles have a rod-like shape. EDAX experiments were performed to identify the composition of the metallic particles and it was found that the particle composed of Pt and Pd in ratio that is comparable to that present in the feed solution, that is (Pt:Pd) (3:1).

Table 3 The electrochemical parameters, corresponding to EIS data for effect of temperature, estimated from the fitting of experimental data to the equivalent circuit of Fig. 10

Temp/°C	R_s	C_{dl}	W	R_2	CPE	n
20	114.5	3.19×10^{-5}	3,389	10,180	164.7	0.29
25	124.2	1.94×10^{-5}	2,937	1,937	121.0	0.20
30	140.2	1.54×10^{-5}	2,492	5,232	197.2	0.24

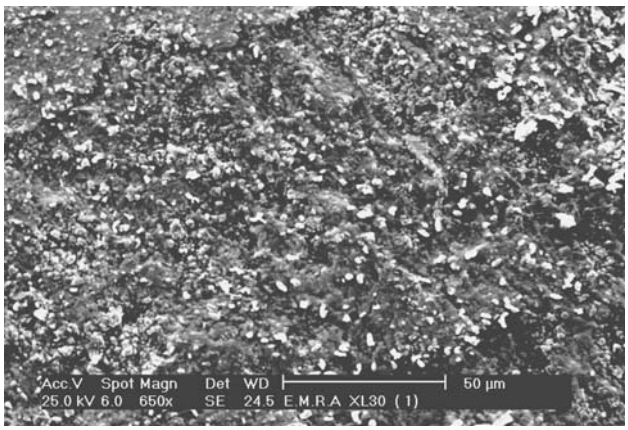

Fig. 11 SEM for copolymer prepared from a feed solution containing (MT:NMPy, 9:1)/0.05 M $TBAPF_6$/AcN, by applying +1.8 V for 1 min, modified with co-catalyst (Pd:Pt, 1:3), ($E_{app.}$ = 100 mV, for 10 min) with magnification 650 times

3.10 TGA of the Modified Polymer Films

Figure 13 shows TGA (a) and DTG (b) data for the polymer and the polymer modified with the submicro/nano-structured Pt/Pd particles. The total weight loss is 65.307% for the polymer and 62.481% for the modified polymer. The weight loss for the modified polymer is smaller than that for the unmodified polymer. It can be concluded that the thermal stability of the polymeric film is increased when modified with the metallic particles.

4 Conclusion

– The polymeric film was employed as a support for sub-micro/nano-structured Pt/Pd alloy and then the

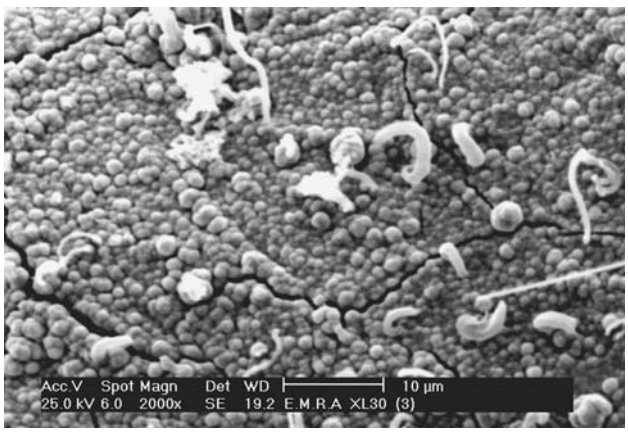

Fig. 12 The same as Fig. 11, with magnification 2,000 times

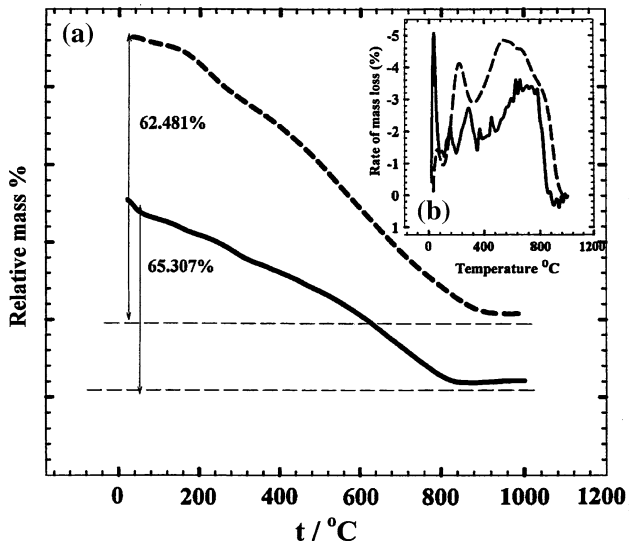

Fig. 13 TGA (**a**) and DTG (**b**) data for copolymer (9:1) (—) and copolymer (9:1) modified with the co-catalyst (- - - -)

resulting hybrid material was used as a catalyst for methanol oxidation.

– Several factors affecting the catalytic efficiency were studied such as:

  - The polymer film thickness: the current of methanol oxidation is relatively higher for thinner films. This can be explained on the basis that as the film thickness increases its electronic resistance increases and should therefore hinder the charge transfer.
  - The amount of catalyst deposited: the catalytic efficiency for methanol oxidation increases with the amount of co-catalyst due to the increase in the surface area of the co-catalyst.
  - The catalyst deposition voltage: the increase in the positive limit of the catalyst deposition voltage results in a decrease in the current due to methanol oxidation, because it results in catalyst oxidation rather than increasing its amount or size.
  - Temperature effect: the current due to methanol oxidation increases with temperature and reaches a maximum at 30 °C then it decays as the adsorption of methanol onto Pt is hindered at higher temperatures.
  - Methanol concentration: as the concentration of methanol increases the oxidation peak current increases with a shift in the positive direction.
  - The co-catalyst composition: the current density increases with the increase of Pd content and then decreases again. The maximum is found when the Pd:Pt ratio is 1:3. Compared to pure Pt, the inclusion of Pd improves the catalytic activity of the catalyst. However, as the increase in the Pd content causes further decrease in the electrocatalytic activity. This is due to the fact that Pd has no catalytic activity for the electrooxidation of methanol.

– The modified film is relatively stable for successive cycling in the acidic methanol up to about 50 cycles. The observed decrease in current value for the oxidation process for the last cycle is about 2% compared to that of the first cycle.
– The best electrolytic efficiency for methanol oxidation was that recorded for the copolymer (9:1) modified with the submicro-/nano-structured catalyst. The "synergistic" effect caused by the polymer film and the catalyst is more pronounced with the copolymer than for PMT.

Acknowledgment The authors are grateful to the University of Cairo (Office of Vice President for Graduate Studies and Research) for providing partial financial support through ''The Young Researchers' Program''.

References

1. Grier DG (1998) MRS Bull 23:21
2. Reetz MT, Quaiser SA, Breinbauer R, Tesche B (1995) Angew Chem Int Ed Engl 34:2728
3. Qi Z, Pickup PG (1998) Chem Commun 28:15
4. Hepel M (1998) J Electrochem Soc 145:124
5. Deki S, Akamatsu K, Yano T, Mizuhata M, Kajinami A (1998) J Mater Chem 8:1865
6. Li Y, Lenigk R, Wu X, Gruending B, Dong S, Renneberg R (1998) Electroanalysis 10:671
7. Lamy C, Léger J-M, Garnier F (1997) In: Nalwa HS (ed) Handbook of organic conductive molecules and polymers. Conductive polymers: spectroscopy and physical properties 3. Wiley, NY, p 471
8. Parsons R, VanderNoot T (1988) J Electroanal Chem 257:9
9. Mikhylova AA, Molodkina EB (2001) J Electroanal Chem 509:119
10. Bouzek K, Mangold KM, Jutter K (2000) Electrochim Acta 46:661
11. Laborde H, Leger JM, Lamy C (1994) J Appl Electrochem 24:219
12. Kost KM, Bartak DE, Kazee B, Kuwana T (1988) Anal Chem 60:2379
13. Strike DJ, De Roou NF, Koudelka-Hep M (1992) J Appl Electrochem 22:922
14. Laborde H, Leger JM, Lamy C, Garnier FC, Yassar A (1990) J Appl Electrochem 20:524
15. Yang H, Lu TH, Xue K, Sun SG, Lu GQ, Chen SP (1997) J Electrochem Soc 144:2302
16. Castro Luna AM (2000) J Appl Electrochem 30:1137
17. Niu L, Li QH, Wei FH, Chen X, Wang H (2003) J Electroanal Chem 544:121
18. Napporn WT, Laborade H, Leger JM, Lamy C (1996) J Electroanal Chem 404:153
19. Laborde H, Leger JM, Lamy C (1994) J Appl Electrochem 24:1019

20. Kelaidopoulou A, Abelidou E, Papoutsis A, Polychroniadis EK, Kokkinidis G (1998) J Appl Electrochem 28:1101
21. Kelaidopoulou A, Papoutsis A, Kokkinidis G (1999) J Appl Electrochem 29:101
22. Vigier F, Gloaguen F, Leger JM, Lamy C (2001) Electrochim Acta 46:4331
23. Lima A, Coutanceau C, Leger JM, Lamy C (2001) J Appl Electrochem 31:379
24. Lenoe A, Marino W, Scharifker BR (1992) J Electrochem Soc 139:438
25. Zhong QL, Li WH, Tian ZQ (1994) Acta Physchim Sin 10:813
26. Zhang H, Wang Y, Fachini ER, Cabrera CR (1999) Electrochem Solid State Lett 2:437
27. Li WS, Tian LP, Huang QM, Li H, Chen HY, Lian XP (2002) J Power Sources 104:281
28. Che GL, Lakshmi BB, Fisher ER, Martin CR (1998) Nature 393:346
29. Parsous R, Vandemoot T (1988) J Electroanal Chem 257:9
30. Roncali J (1997) Chem Rev 97:173
31. Rehbach MS (1994) Pure Appl Chem 66:1831
32. Dubois M, Billand D (2002) Electrochim Acta 47:4459
33. Tanguy J, Baudoin JL, Chao F, Costa M (1992) Electrochim Acta 37:1417
34. Bobacka J, Ivaska A, Grzeszczuk M (1991) Synth Met 44:21
35. Tourillon G, Garnier F (1982) J Electroanal Chem 135:173